# Steady-state exhumation pattern in the Central Andes SE Peru

G. M. H. Ruiz, V. Carlotto, P. V. Van Heiningen and P. A. M. Andriessen

*Geological Society, London, Special Publications* 2009; v. 324; p. 307-316
doi:10.1144/SP324.20

# Steady-state exhumation pattern in the Central Andes – SE Peru

G. M. H. RUIZ[1,2]*, V. CARLOTTO[3], P. V. VAN HEININGEN[1] & P. A. M. ANDRIESSEN[1]

[1]*Vrije Universiteit (Vu), Amsterdam, The Netherlands*

[2]*Present address: University of Neuchâtel, Neuchâtel, Switzerland*

[3]*INGEMMET, Lima, Peru*

**Corresponding author (e-mail: geoffrey.ruiz@unine.ch)*

**Abstract:** The Western Cordillera of SE Peru is part of the Central Andes and is situated to the west of the Eastern Andes from which it is separated by the northern termination of the Altiplano – the Inter-Andean Valley. It is a volcanic–volcano-detrital chain that developed in the Palaeogene, and is characterized by a 4000 m-high mean altitude whose origin is poorly constrained. We selected a vertical profile in the region of Abancay to trace the record the evolving uplift and erosion history of the Andean orogen. Fission-track data on both apatite and zircon crystals were completed on plutonic rocks of the Tertiary Andahuaylas–Yauri batholith. Ages ranged between 24 and 14 Ma, and 38 and 30 Ma, respectively. Thermal modelling was completed for the whole profile and does not, like age–altitude relationships, show evidence of any clear disruption of the exhumation paths since 38 Ma either by sedimentary burial and/or rapid exhumation. One of the noteworthy aspects of the data is that exhumation was steady at a rate of 0.17 km $Ma^{-1}$ from the late Eocene until at least the middle Miocene (38–14 Ma). The uplift of the Western Cordillera was thus probably steady for this period with sedimentary deposition restricted to the present-day Altiplano and Inter-Andean Valley regions.

The uplift chronology of the Central Andes is contentious (Gregory-Wodzicki 2000; Lamb & Davis 2003; Ghosh *et al.* 2006; Garzione *et al.* 2006, 2008; Sempere *et al.* 2006; Hartley *et al.* 2007). It is currently considered that deformation and uplift began in the Western Cordillera (WC) in the Eocene, developed later and more slowly in the Eastern Cordillera (EC) (40–10 Ma: McQuarrie *et al.* 2008), whereas the Subandean Zone (SAZ) probably developed as early as the Middle Miocene (Barnes *et al.* 2008; McQuarrie *et al.* 2008). Phases of deformation and uplift are often constrained by lateral association with Bolivia further south, with the exception of two recent studies from the WC further south that demonstrated that it was affected in the Late Miocene by a phase of uplift (Schildgen *et al.* 2007; Thouret *et al.* 2007). Palaeomagnetic and $^{40}Ar/^{39}Ar$ studies (Gilder *et al.* 2003; Rousse *et al.* 2003, 2005) indicate that major mountain building developed 12–10 Ma ago in the EC coevally with ridge subduction and transpressional deformation in the Altiplano region. Additional palaeomagnetic data indicate that counter-clockwise rotation probably occurred earlier, i.e. before 15 Ma, in the fore-arc region between Bolivia and Peru (Roperch *et al.* 2006), and as early as the late Eocene–early Oligocene in the northern termination of the Altiplano in SE Peru (Roperch *et al.* 2008). Establishing long-term order rates and patterns of mountain exhumation, both among and within individual ranges, is therefore a high priority. Thermochronology is an indispensable tool for such studies and fission-track dating is the best of all methods because of its associated thermal modelling, but also because it allows an immediate and reliable estimation of exhumation through an internal pair method on apatite and zircon minerals.

We complement and add to the previous studies by presenting the first apatite (AFT) and zircon (ZFT) fission-track thermochronological ages from a vertical profile located in the Western Cordillera of southern Peru near the town of Abancay (Fig. 1). The apatite partial annealing zone (APAZ) and zircon (ZPAZ) in the fission-track system lies between 60–120 °C (Green *et al.* 1989) and 210–270 °C (Tagami *et al.* 1996). Hence, it is particularly useful for evaluating low-temperature thermal histories, i.e. those affecting the upper 8–10 km of the WC, depending on the geothermal gradient. We have chosen this part of the WC because it exhibits: (1) crystalline rocks potentially rich in apatite and zircon; and (2) high slope gradients. Eight bedrocks were sampled along a vertical profile, with an average incremental difference in altitude of 150 m. Results indicate that exhumation was slow and steady since the Late Eocene with no evidence of a recent change,

*From*: LISKER, F., VENTURA, B. & GLASMACHER, U. A. (eds) *Thermochronological Methods: From Palaeotemperature Constraints to Landscape Evolution Models*. Geological Society, London, Special Publications, **324**, 307–316.
DOI: 10.1144/SP324.20 0305-8719/09/$15.00 

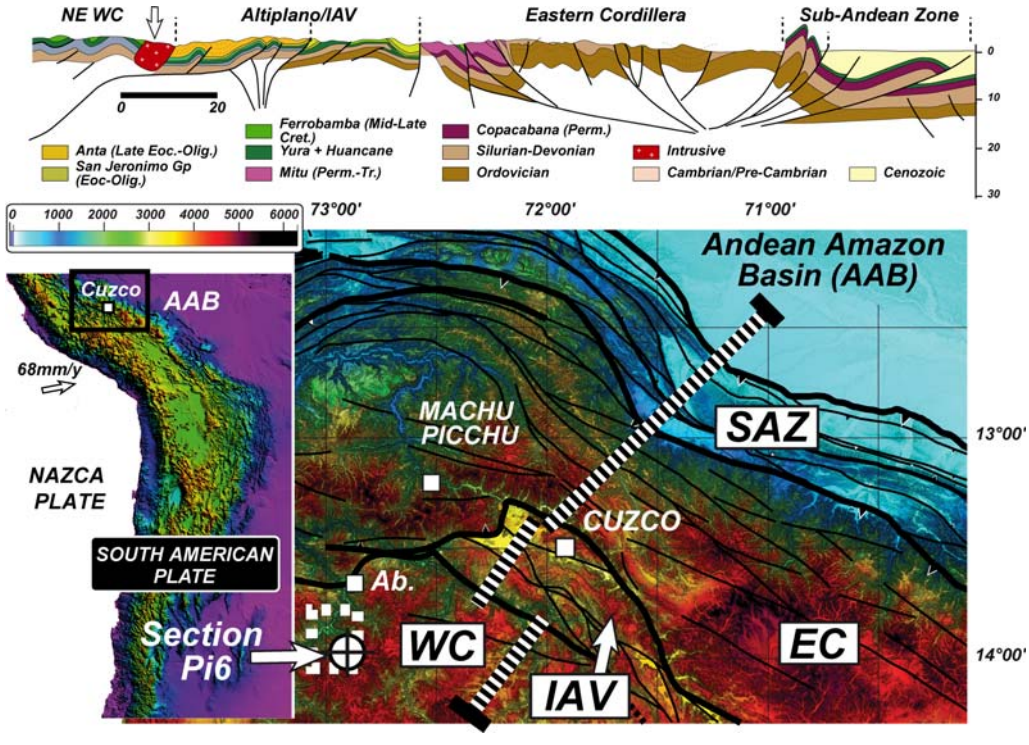


**Fig. 1.** Morphotectonic map of the Central Andes in southern Peru with Nazca–South American plate convergence (Norabuena *et al.* 1999). Location map in a DEM (Digital Elevation Model) from South America (Cornell Universtiy) showing the extent of the studied areas. The thick black lines correspond to boundaries between the different morphotectonic domains: the Andean Amazon Basin (AAB), the Sub-Andean Zone (SAZ), the Eastern Cordillera (EC), the Inter-Andean Valley (IAV) and, finally, the Western Cordillera (WC). Pi6, vertical profile sampled for fission-track analysis in the Andahuaylas–Yauri batholith. Thin black lines, faults. Thick dashed white and black lines, section illustrated to the top (Carlotto 2006). Ab., town of Abancay.

which is very different from earlier records from the Western Cordillera (Schildgen *et al.* 2007; Thouret *et al.* 2007).

## Geodynamic setting

The tectonic framework is as uniform as can be expected over such a large area. The Andes are thrust southeastwards over the South American craton, whereas the subduction of the oceanic Nazca plate, with the buoyant Nazca ridge on top (Hampel 2002; Espurt *et al.* 2007; Clift & Ruiz 2008), beneath the South American plate occurs further west at a rate of 68 mm year$^{-1}$ and towards the ENE (Norabuena *et al.* 1999) (Fig. 1). The Andes in the region of Cuzco–Abancay mark a clear SW–NE offset in the strike of the Andes (Fig. 1) that corresponds to the NW termination of the Bolivian orocline (Fig. 1). The Andes in this area comprise of two different mountain ranges, the Eastern (EC) and Western (WC) Cordilleras, each having an elevation greates than 6000 m and separated by the 3800 m-high northern termination of the Altiplano, i.e. the Inter-Andean Valley (IAV; Fig. 1).

The WC is a volcanic–volcano-detrital chain that developed approximately 40–50 Ma ago (Jaillard *et al.* 2000) and is still characterized by 5000–6500 m-high active volcanoes that disappear north of about 14–15°S. Parts of the WC are composed of Tertiary plutons, such as the Andahuaylas–Yauri batholith in the region of Abancay (Fig. 2) (Noble *et al.* 1984; Perello *et al.* 2003). Earlier evolution, i.e. late Permian–middle Jurassic, corresponds to lithospheric thinning and a phase of rifting, whereas marine–alluvial sedimentation took place in the WC from middle Jurassic to middle Cretaceous (Sempere *et al.* 2002). Thickening and loading of the crust beneath the WC resulted in the development of a Palaeocene–Eocene foreland basin with continental deposits at the boundary zone between the WC and the Altiplano (Carlotto *et al.* 2005). Early Eocene sedimentation is not preserved in the WC, but exists in the IAV near Cuzco

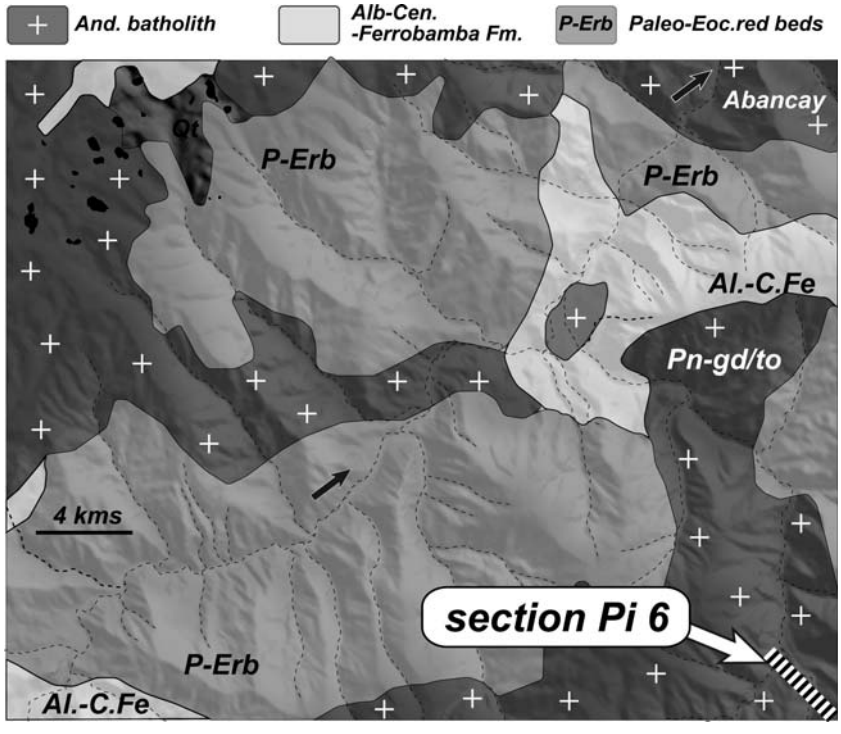


**Fig. 2.** Geological map (modified from INGEMMET) of the studied area with the sample site (bottom right) on top of a 90 m-resolution DEM (CGIAR-CSI). Dashed thin black lines, rivers; And., Andahuaylas–Yauri.

with a 5 km-thick pile of continental series deposits. The scope of this paper is not a complete structural and stratigraphic study, so for further details the reader should refer to Laubacher (1978), Carlotto (1998) and Sempere *et al.* (2002).

## Results and interpretation

### *Zircon fission-track (ZFT) data*

ZFT ages range between $36.1 \pm 1.8$ and $31.3 \pm 1.6$ Ma, whereas all data pass $\chi^2$ test (Gailbraith 1981) (Table 1), suggesting non-dispersion in individual grain ages. ZFT ages are older towards the top of the section and younger towards the bottom (Fig. 3), suggesting that all samples belong to a thermally homogeneous block that cooled through the ZPAZ in the late Eocene–early Oligocene. Such a phase post-dated the Early–Middle Eocene age of intrusion for this batholith (Noble *et al.* 1984; Perello *et al.* 2003).

### *Apatite fission-track (AFT) data*

AFT ages are younger than ZFT ages, and comprised ages between $22.5 \pm 1.9$ and $15.5 \pm 1.5$ Ma (Table 1 and Fig. 3). Between 21 and 46 track lengths were measured per sample, with mean values varying between 11.20 and 14.04 μm; whereas standard deviation (SD) and $D_{par}$ (Ketcham *et al.* 1999) measurements range between 1.9 and 0.8 μm, and 2.37 and 2.98 μm, respectively (Table 1 and Fig. 4). Mean track lengths (MTL) and SD are plotted v. age (Fig. 4): no clear pattern of long track length and short SD is visible, thus indicating that this part of the WC did not undergo any rapid phase of cooling through the 120–60 °C temperature window. In addition, track-length distributions are roughly unimodal (Fig. 5), corroborating that these samples underwent a simple phase of slow cooling between 120 and 60 °C.

### *Temperature–time modelling*

Inverse temperature–time modelling was performed for all samples from bottom to top of the profile using the AFTsolve program (Ketcham *et al.* 2000). Input parameters for modelling are AFT ages, track lengths and $D_{par}$ distributions, as well as ZFT ages and geological constraints, such as the imposed presence near the surface at a given time. Two sets of thermal modelling were

**Table 1.** *Apatite fission-track (AFT) and zircon fission-track (ZFT) ages from the Andahuaylas–Yauri batholith in the Western Cordillera of southern Peru (Figs 1 & 3)*

| ID | Altitude (m) | Lat. | Long. | *N* | $P\chi^2$ (%) | $\rho_s$ ($N_s$) ($\times 10^6$) | $\rho_i$ ($N_i$) ($\times 10^6$) | $\rho_d$ ($N_d$) ($\times 10^6$) | Age (Ma) | $\pm 1\sigma$ (Ma) | U (ppm) | MTL (μm) | SD | $D_{par}$ (μm) | SD |
|---|---|---|---|---|---|---|---|---|---|---|---|---|---|---|---|
| Apatite | | | | | | | | | | | | | | | |
| Pi6.1 | 3870 | −13.9853 | −72.8747 | 23 | 10.0 | 2.274 (456) | 20.740 (4159) | 11.015 (6155) | 22.5 | 1.9 | 23.37 | 11.21 ± 0.34 (41) | 1.9 | 2.68 ± 0.22 (40) | 0.25 |
| Pi6.2 | 3800 | −13.9833 | −72.8737 | 16 | 100.0 | 1.554 (168) | 13.793 (1491) | 10.907 (6155) | 22.0 | 1.9 | 16.87 | 13.40 ± 0.23 (31) | 1.3 | 2.78 ± 0.29 (20) | 0.32 |
| Pi6.3 | 3650 | −13.9806 | −72.8746 | 20 | 99.5 | 1.741 (323) | 16.199 (3005) | 10.798 (6155) | 20.8 | 1.4 | 17.88 | 14.04 ± 0.16 (37) | 1.0 | 2.87 ± 0.20 (44) | 0.24 |
| PI6.4 | 3450 | −13.9790 | −72.8772 | 20 | 98.0 | 0.685 (137) | 6.210 (1242) | 10.690 (6155) | 21.1 | 2.0 | 7.07 | 12.76 ± 0.21 (46) | 1.4 | 2.37 ± 0.21 (28) | 0.23 |
| Pi6.5 | 3250 | −13.9759 | −72.8815 | 19 | 100.0 | 0.787 (148) | 9.048 (1701) | 10.582 (6155) | 16.5 | 1.5 | 10.44 | 13.13 ± 0.18 (34) | 1.1 | 2.55 ± 0.23 (43) | 0.35 |
| Pi6.6 | 3100 | −13.9735 | −72.8810 | 20 | 87.0 | 1.036 (203) | 12.010 (2354) | 10.474 (6155) | 16.2 | 1.3 | 13.96 | 13.36 ± 0.17 (21) | 0.8 | 2.61 ± 0.27 (31) | 0.29 |
| Pi6.7 | 3000 | −13.9727 | −72.8853 | 20 | 93.0 | 1.092 (141) | 12.680 (1637) | 10.366 (6155) | 16.0 | 1.5 | 16.25 | 12.89 ± 0.26 (35) | 1.6 | 2.72 ± 0.22 (23) | 0.29 |
| Pi6.8 | 2850 | −13.9680 | −72.8941 | 20 | 93.0 | 0.862 (140) | 10.228 (1662) | 10.258 (6155) | 15.5 | 1.5 | 12.48 | 12.45 ± 0.21 (30) | 1.1 | 2.98 ± 0.31 (17) | 0.30 |
| Zircon | | | | | | | | | | | | | | | |
| Pi6.1 | 3870 | −13.9853 | −72.8747 | 19 | 47.0 | 7.771 (1088) | 8.436 (1181) | 6.485 (7200) | 36.1 | 1.8 | 51.08 | 8.69 ± 0.32 (11) | 1.1 | – | – |
| Pi6.2 | 3800 | −13.9833 | −72.8737 | 20 | 71.0 | 10.811 (1287) | 11.719 (1395) | 6.379 (7200) | 35.5 | 1.7 | 76.41 | 9.70 ± 0.48 (5) | 1.0 | – | – |
| Pi6.3 | 3650 | −13.9806 | −72.8746 | 19 | 96.0 | 13.627 (1146) | 14.828 (1247) | 6.274 (7200) | 34.8 | 1.7 | 96.34 | – | – | – | – |
| Pi6.4 | 3450 | −13.9790 | −72.8772 | 17 | 32.0 | 20.555 (3443) | 22.322 (3739) | 6.168 (7200) | 34.93 | 1.2 | 163.15 | – | – | – | – |
| Pi6.5 | 3250 | −13.9759 | −72.8815 | 20 | 55.0 | 14.403 (3356) | 15.562 (3626) | 6.063 (7200) | 33.8 | 1.2 | 110.33 | – | – | – | – |
| Pi6.6 | 3100 | −13.9735 | −72.8810 | 20 | 66.0 | 18.809 (4493) | 20.857 (4982) | 5.957 (7200) | 32.4 | 1.1 | 143.63 | – | – | – | – |
| Pi6.7 | 3000 | −13.9727 | −72.8853 | 20 | 97.0 | 10.108 (2153) | 11.028 (2349) | 5.757 (7200) | 31.9 | 1.3 | 76.83 | – | – | – | – |
| Pi6.8 | 2850 | −13.9680 | −72.8941 | 20 | 59.0 | 14.242 (2009) | 15.816 (2231) | 5.746 (7200) | 31.3 | 1.6 | 109.58 | 9.79 ± 0.30 (11) | 1.0 | – | – |

Apatite and zircon separates were counted by G.M.H. Ruiz using $\zeta'$calibration factors of 359 ± 11 (CN5 standard glass, 1250× magnification) and 121 ± 3 (CN1 standard glass, 1600× magnification-oil), respectively, and irradiated at the Petten facility. Apatites were etched in 5.5 M $HNO_3$, at 21 °C for 20 s (Carlson *et al.* 1999), whereas zircons were etched in a eutectic melt of NaOH–KOH at 220 °C (Gleadow *et al.* 1976). Numbers in parentheses indicate the number of measured track lengths (MTL) and $D_{par}$. (Ketcham *et al*. 1999) values. *N*, number of dated grains per sample; SD, standard deviation. The time–temperature modelling of sample Pi6.6 was not completed because of the small number of track-length measurements (21).

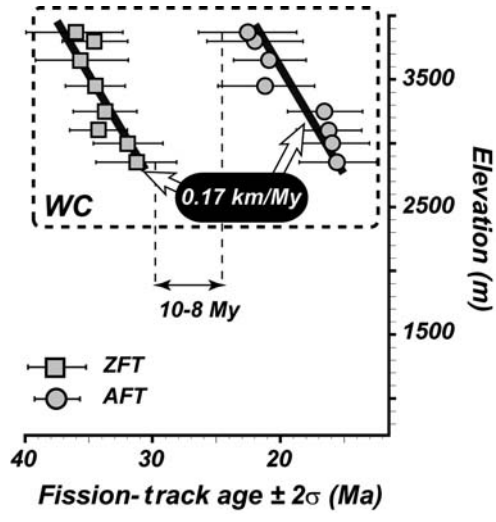


**Fig. 3.** AFT and ZFT age–altitude plots from the Andahuaylas–Yauri batholith in the Western Cordillera (WC). Fission–track ages for both apatite and zircon gets younger towards the bottom of the profiles (Table 1). Grey lines, best correlation fit paths within $2\sigma$ error bars.

performed, one without any geological constraints – modelling 'free' (Fig. 5, left) – and one with an imposed presence at/or near the surface in about the early Oligocene (Fig. 5, right) because of the presence of continental sediments (Anta Formation) on top of the batholith in the IAV to the south of Cuzco (Carlotto *et al.* 2005).

Temperature–time models for the first set indicate that the upper sample (Pi6.1) entered the apatite partial annealing zone (APAZ, 120–60 °C) at about 30 Ma, whereas the bottom sample (Pi6.8) entered approximately 20 Ma ago (Fig. 5, right). Similarly, the uppermost sample left the APAZ about 18–20 Ma ago, about the same time as the lowermost sample entered it, and the lowermost sample left the zone in the last 5 Ma.

The second set of models yielded good-quality Kolmogorov–Smirnov (K–S) tests, such as the first one giving results of between 0.64 and 0.93, and 0.72 and 0.98, respectively (Fig. 5). Thermal modelling for the six lowermost samples suggest a total resetting to a temperature greater than 120 °C in the late Oligocene–early Miocene, whereas a less protracted phase of heating is modelled for the two upper ones (Fig. 5, right). Such a phase was followed by a phase of cooling starting from about

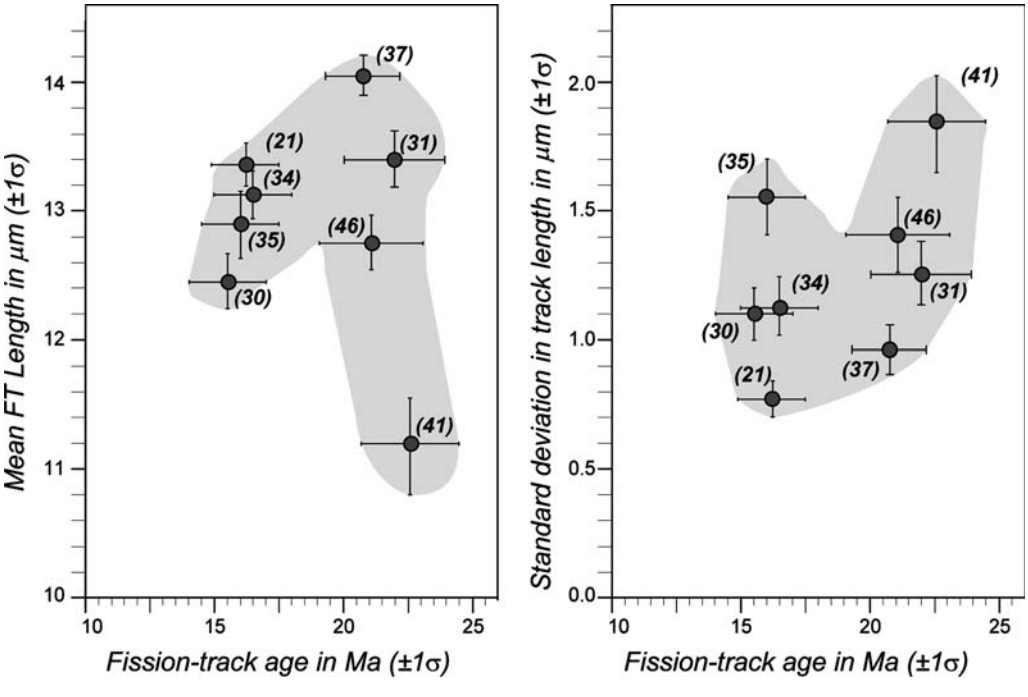


**Fig. 4.** Relationship between the AFT age and the mean track length (left), and standard deviation (right) – section Pi6. The relationship is shown for all samples that yielded adequate track length data (all errors are $\pm 1\sigma$). Shading shows the general trend of the data.

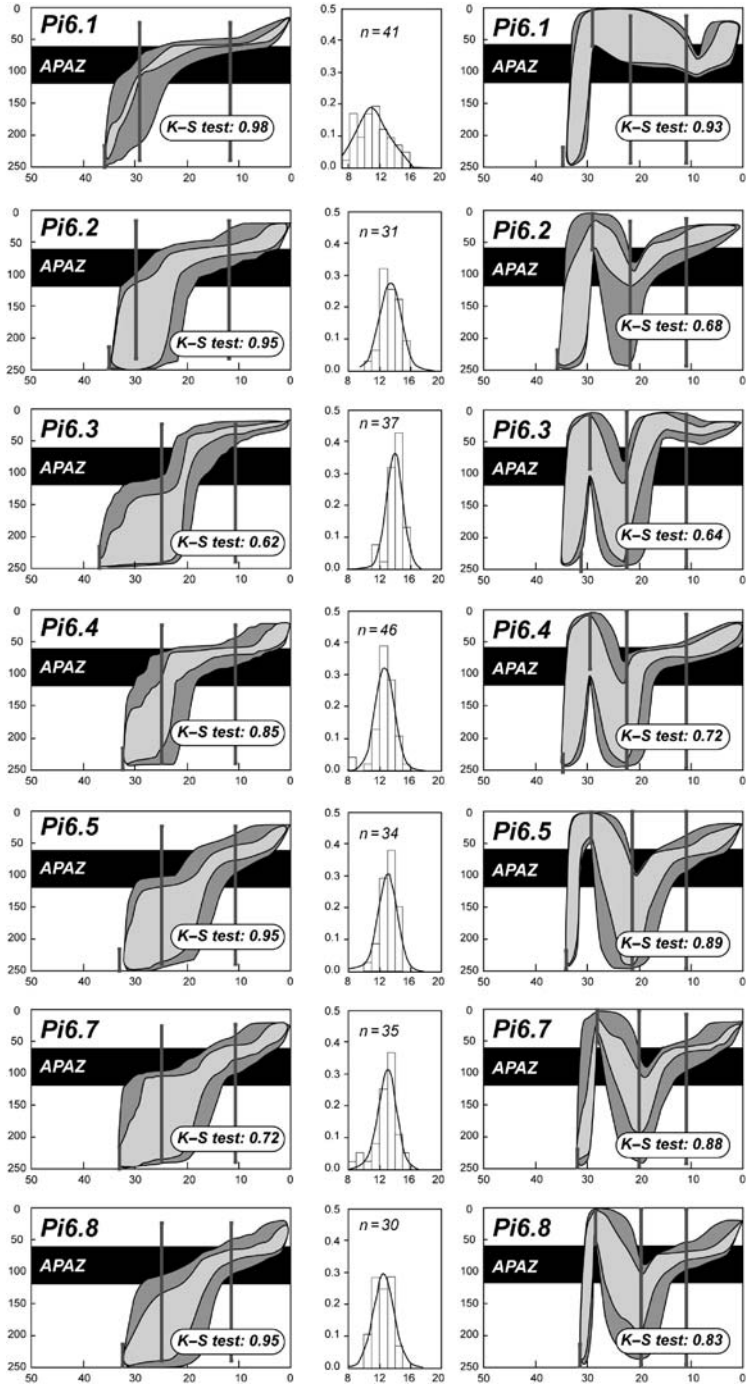


**Fig. 5.** Temperature–time ($T$–$t$) modelling of seven samples from the Andahuaylas–Yauri batholith (see Figs 1 & 2 for the locations, and Table 1 for details). $T$–$t$ modelling was completed following the procedures described in Ketcham *et al.* (2000) with geological and temperature (ZFT ages) constraints (vertical grey bars). (Left) Modelling 'free' (see text), i.e. without any geological constraints. (Right) Models with an imposed near-surface presence in the early Oligocene (vertical grey bar). (Middle) Track-length histogram ($X$-axis, length in μm; $Y$-axis, relative representation; $n$, number of measured confined tracks). The best $T$–$t$ paths fitting both the AFT age and the track-length distribution (right) and the Kolmogorov–Smirnov (K–S) test are shown: dark (65%) and light (95%) confidence. APAZ, apatite partial annealing zone.

20 Ma until 17–16 Ma. The most recent thermal history cannot be constrained because models are outside, or at the upper edge, of the 120–60 °C (APAZ) temperature window, with the exception of the bottom sample (Pi6.8; Fig. 5, right), which points towards a loosely constrained and ultimate phase of cooling starting at around 5–4 Ma.

Differences between the two sets of models are roughly restricted for most of the samples in the left-hand part of the models, i.e. pre-24–20 Ma (Fig. 5), and correspond to the the geological constraint we added. Models were forced to reach temperatures lower than 60 °C, i.e. the near surface at *c.* 31–28 Ma, but had time to reach temperatures of at least 120 °C, i.e. total resetting, before models of the first set enter the APAZ (Fig. 5). The two thermal models for the uppermost sample (Pi6.1) do not have any similarity because the early entrance into the APAZ for the first set is anterior to, or almost synchronous with, its near-surface position in the second one. Hence, these two models are much contrasted, with a clear phase of cooling starting at arount 10–9 Ma for the second set (Fig. 5, right). This late phase of cooling is absent from lower samples where no fault system exists between sample sites. All this suggests that the true time–temperature paths for this part of the Western Cordillera most probably correspond to the ones yielded by the first configuration, i.e. without: (1) any near-surface presence in the late Eocene–early Oligocene; and (2) rapid and important burial in the late Oligocene–early Miocene.

### *Age–elevation plots*

AFT and ZFT ages are plotted v. altitude (Fig. 3). Slopes and age differences from bottom to top of the profile are almost identical for the two thermochronometers, pointing towards an apparent exhumation rate of about 0.17 km $Ma^{-1}$ between 36 and 31 Ma (ZFT), and 23 and 15 Ma (AFT). This rate is low and in agreement with the periods of slow cooling we evidenced through the APAZ (120–60 °C) by thermal modelling (Fig. 5, left). Hence, we are confident that exhumation was slow and at a rate of 0.1–0.2 km $Ma^{-1}$ in this region of the WC for these two periods.

## Discussion and conclusions

### *Late Eocene–Oligocene*

The late Eocene–Early Oligocene epoch was characterized by a period of slow exhumation in the WC near Abancay (Fig. 1), as evidenced by thermal modelling and ZFT age–altitude relationships (Figs 3 & 5). This period most probably postponed the emplacement of the Andahuaylas–Yauri batholith of Eocene age (Noble *et al.* 1984; Perello *et al.* 2003) until shallow crustal levels. Some K/Ar data exist from the Eastern Cordillera 150 km further to the NE (Farrar *et al.* 1988; Kontak *et al.* 1990*a*, *b*) that are interpreted as reflecting the development of a NW-oriented tectono-thermal zone in relation to an important phase of mountain building at approximately 38 Ma. Such as event would correspond to the so-called Incaic phase of Steinmann (1929), which was related in the 1990s to a change towards rapid convergence between the South American and Farallon plates (Mégard 1984; Pardo-Casas & Molnar 1987). This phase of deformation can probably be traced in the WC of southern Peru through shortening (Carlotto 2006), but was not associated with rapid (as evidenced by thermal modelling) nor important exhumation because late Eocene ZFT ages are still present today at the surface. As previously stated the subsection on 'Temperative–time modelling', a 5000–6000 m-thick pile of late Eocene–middle Oligocene syn-orogenic sediments has been reported in the IAV near Cuzco (Carlotto 1998; Carlotto *et al.* 2005). Such a pile is absent today in the WC, suggesting either non-deposition or post-depositional erosion in the WC. If deposited where our profile was selected, this pile would have been heated by sedimentary burial of the Andahuaylas–Yauri batholith to the extent of 5.5 km × 25 °C $km^{-1}$, i.e. *c.* 137.5 °C, as illustrated on the right-hand side of Figure 5. However, we reject the post-depositional erosion solution because time–temperature modellings are not consistent from the bottom to the top of the profile (see earlier).

All combined data suggest that the IAV was most probably limited to the west in the Eocene–Oligocene by the slowly exhuming WC, and possibly (because quantitative constraints are still poor) to the east by a developing Eastern Cordillera.

### *Miocene*

Exhumation occurred at a similar rate of 0.17 km $Ma^{-1}$ for the early Miocene (22–15 Ma ) and late Eocene–Early Oligocene in the WC, whereas a gap of 9 Ma prevails between the two periods (Fig. 3). We interpret this time lag to correspond to the temperature gap between the partial annealing zones of the zircon and apatite systems because a total resetting to temperatures of more than 120 °C at a time between the two periods is unlikely (see the previous subsection). An identical rate for these two epochs is thus not a coincidence but rather characterized a sole and continuous phase of exhumation from about 36 to 15 Ma.

Different basins of Eocene–Miocene age existed in the IAV (Fig. 1). Clasts indicate that source rocks

were mainly composed of quartzites, carbonates, volcanics and plutonic rocks (see the compilation in Carlotto *et al.* 2005). Carbonate and quartzite clasts were probably sourced from sediments that constituted Mesozoic basins in the present-day EC and WC (Sempere *et al.* 2002), whereas volcanic activity prevailed in the region from at least 40 Ma (see the next subsection). Clasts of plutonic origin are only encountered in adjacent basins to the NE of the Andahuaylas–Yauri batholith (e.g. Descanso Basin: Carlotto *et al.* 2005) from the Middle to Late Miocene, suggesting that the upper levels of the batholith reached the surface not before the Middle Miocene. This additional evidence is in total agreement with the slow phase of cooling we modelled for the middle–late Miocene (Fig. 5, left). Since deposition in the Miocene, shortening from 45% to 25% occurred in the IAV, which was constrained by surface data (Carlotto 2006).

### *Palaeo-geothermal gradient*

Our pair fission-track ages indicate that exhumation was continuous and at a rate of 0.17 km $Ma^{-1}$ from *c.* 35 until 15 Ma. A palaeo-geothermal gradient can be deduced from these analyses using the following formula:

$$G = \frac{\Delta T}{\Delta l} = \frac{T_c(\mathrm{ZFT}) - T_c(\mathrm{AFT})}{\Delta l}$$

where $T_c$(ZFT) and $T_c$(AFT) are the temperatures of closure of the AFT and ZFT systems that can be approximated to 230 and 110 °C, respectively (Reiners & Brandon 2006). $\Delta l$ is an artificial depth that we calculate using the exhumation rate of 0.17 km $Ma^{-1}$, and the almost identical (within error bars) age difference, $\Delta t$, of *c.* 14–15 Ma we produced using the AFT and ZFT systems from a single sample, e.g. the lowermost (Pi6.8) or the uppermost one (Pi6.1: Fig. 3 and Table 1):

$$\Delta l = \frac{\Delta l}{\Delta t} \times \frac{\Delta t}{1} = 0.17 \times 15 = 2.55 \text{ km}.$$

In turn, the geothermal gradient becomes:

$$G = \frac{\Delta T}{\Delta l} = \frac{230 - 110}{2.55} = 47\ ^\circ\mathrm{C\ km^{-1}}.$$

A value of 47 °C $km^{-1}$ is high but in the perfect range of geothermal gradients for the upper 12 of the crust in the Andes, and more generally in volcanic arcs (Henry & Pollack 1988). The geothermal gradient we calculated most probably prevailed from 36 Ma, i.e. the ZFT age of the uppermost sample, until about 15 Ma, i.e. the AFT age of the lowermost dated level, suggesting continuous volcanic activity in this region until at least 15 Ma, which is corroborated by the presence of volcanic levels in most of the neighbouring Eocene–Late Miocene basins (Carlotto *et al.* 2005).

### *Uplift of the Western Cordillera of southern Peru*

The depth of closure for the ZFT system depends on the geothermal gradient. Using the geothermal gradient we calculated for the Late Eocene–Middle Miocene of approximately 47 °C $km^{-1}$, the depth of closure corresponds to 230/47, i.e. *c.* 5 km. Bedrocks from the Andahuaylas–Yauri batholith today yield late Eocene ZFT ages suggesting that denudation has not exceeded 5 km since. Interestingly, the WC is today characterized by a mean altitude of 3500–4000 m to the south of Abancay (Fig. 1). This prompts the question: when did the WC acquire its topography? Our results suggest: (1) a continuous exhumation from the late Eocene until the middle Miocene, independent of the high contemporaneous geothermal gradient that prevailed in this region of the Central Andes; and (2) there has been no phase of heating/burial since the late Eocene for the Andahuaylas–Yauri batholith near Abancay. We thus favour a model involving continuous uplift from at least the late Eocene with sediment deposition in basins located today in the IAV, which was later tightened up in the middle to late Miocene (Carlotto 1998, 2005, 2006; Rousse *et al.* 2003, 2005). The locus of deformation has since been transferred along the foothills of the Andes in SE Peru (Hermoza 2004), which yield very young AFT ages (Fig. 3). The possible causes are many and possibly coupled, these are: (a) the westward drift of the South American plate (Russo & Silver 1996); (b) the thickening of the crust (Isacks 1988); (c) the sediment starvation along the trench because of aridity in the fore-arc (Hartley 2003); and (d) the ridge subduction below the South American plate (Hampel 2002; Rousse *et al.* 2003; Espurt *et al.* 2007, 2008; Clift & Ruiz 2008); the latter two increasing friction between the subducting Nazca and South American plates (Lamb & Davis 2003), and transferring shortening within the interior of the South American plate (Espurt *et al.* 2008).

However, whatever processes are considered to have shaped the geology of SE Peru, none generated rapid exhumation in the Western Cordillera near Abancay from the Late Eocene until the Middle Miocene. The exhumation pattern is rather slow and steady for this period, at a rate of about 0.17 km $Ma^{-1}$, whereas the post-middle Miocene record would probably be traceable using a

thermochronometer with a lower temperature of closure, i.e. U–Th/He on apatite (70 °C: Farley 2000), similar to what was undertaken further south by Schildgen *et al.* (2007) to ascribe a late Miocene age for the uplift of the western margin of the Andean plateau.

We wish to thank A. Hartley, B. Ventura, D. Seward and F. Lisker for constructive reviews; J. Jacay, T. Sempere, E. Jaillard and P. Roperch for discussions on the regional geology; and J. Salichon and M. Ruiz for field-work assistance.

## References

BARNES, J. B., EHLERS, T. A., MCQUARRIE, N., O'SULLIVAN, P. B. & TAWACKOLI, S. 2008. Thermochronometer record of central Andean plateau growth, Bolivia (19.5S). *Tectonics*, **27**, TC3003, doi:10.1029/2007TC002174.

CARLOTTO, V. 1998. *Evolution Andine au niveau de Cuzco (Pérou)*. PhD thesis, University of Grenoble, France.

CARLOTTO, V. 2006. El acortamiento y la deformación Andina en el Sur del Perú: Cusco–Abancay–Sicuani. *Boletín Sociedad Geológica del Perú*, **101**, 91–119.

CARLOTTO, V., JAILLARD, E. *ET AL*. 2005. Las Cuencas Terciarias sinorogénicas en el Altiplano y la Cordillera Occidental del Sur del Perú. *Boletín Especial Alberto Giesecke Matto, Sociedad Geológica del Perú*, **6**, 103–126.

CARLSON, W. D., DONELICK, R. A. & KETCHAM, R. A. 1999. Variability of apatite fission-track annealing kinetics: I. Experimental results. *American Mineralogist*, **84**, 1213–1223.

CLIFT, P. D. & RUIZ, G. M. H. 2008. How does the Nazca Ridge subduction influence the modern Amazonian foreland basin? Comment. *Geology*, **36**, doi: 10.1130/G24355C.1.

ESPURT, N., BABY, P. *ET AL*. 2007. How does the Nazca Ridge subduction influence the modern Amazonian foreland basin? *Geology*, **35**, 515–518.

ESPURT, N., FUNICIELLO, F., MARTINOD, J., GUILLAUME, B., REGARD, V., FACENNA, C. & BRUSSET, S. 2008. Flat subduction dynamics and deformation of the South American plate: Insights from analog modeling. *Tectonics*, **27**, TC3011, doi:10.1029/2007TC002175.

FARLEY, K. A. 2000. Helium diffusion from apatite: general behaviour as illustrated by Durango fluorapatite. *Journal of Geophysical Research*, **105**(B2), 2903–2914.

FARRAR, E., CLARK, A. H., KONTAK, D. J. & ARCHIBALD, D. A. 1988. The Zongo–San Gaban zone: eocene foreland boundary of the central Andean orogen, northwest Bolivia and southeast Peru. *Geology*, **16**, 55–58.

GAILBRAITH, R. F. 1981. On statistical models for fission tracks counts. *Mathematical Geology*, **13**, 471–478.

GARZIONE, C. N., HOKE, G. D. *ET AL*. 2008. Rise of the Andes. *Science*, **320**(5881), 1304–1307.

GARZIONE, C. N., MOLNAR, P., LIBARKIN, J. C. & MACFADDEN, B. J. 2006. Rapid late Miocene rise of the Bolivian Altiplano: evidence for removal of mantle lithosphere. *Earth and Planetary Science Letters*, **241**(3–4), 543–556.

GHOSH, P., GARZIONE, C. N. & EILER, J. M. 2006. Rapid uplift of the Altiplano revealed through $^{13}C-^{18}O$ bonds in paleosol carbonates. *Science*, **311**, 511–514.

GILDER, S., ROUSSE, S., FARBER, D., MCNULTY, B., SEMPERE, T., TORRES, V. & PALACIOS, O. 2003. Post-Middle Oligocene origin of paleomagnetic rotations in the Upper Permian to Lower Jurassic rocks from northern and southern Peru. *Earth and Planetary Sciences Letters*, **210**, 233–248.

GLEADOW, A. J. W., HURFORD, A. J. & QUAIFE, R. D. 1976. Fission-track dating of zircon: improved etching techniques. *Earth and Planetary Science Letters*, **33**, 273–276.

GREEN, P. F., DUDDY, I. R., LASLETT, G. M., HEGARTY, K. A., GLEADOW, A. J. W. & LOVERING, J. F. 1989. Thermal annealing of fission tracks in apatite – Qualitative modelling techniques and extensions to geological timescales. *Chemical Geology*, **79**, 155–182.

GREGORY-WODZICKI, K. M. 2000. Uplift history of the Central & Northern Andes: a review. *Geological Society of America Bulletin*, **112**, 1091–1105.

HAMPEL, A. 2002. The migration history of the Nazca Ridge along the Peruvian active margin: a re-evaluation. *Earth and Planetary Sciences Letters*, **203**, 665–679.

HARTLEY, A. J. 2003. Andean uplift and climate change. *Journal of the Geological Society, London*, **160**, 7–10.

HARTLEY, A., SEMPERE, T. & WORNER, G. 2007. A comment on 'Rapid late Miocene rise of the Bolivian Altiplano: Evidence for removal of mantle lithosphere' by C. N. Garzione *et al.* [Earth and Planetary Sciences Letters, **241**(2006), 543–556]. *Earth and Planetary Sciences Letters*, **259**, 625–629.

HENRY, S. G. & POLLACK, H. N. 1988. Terrestrial heat flow above the Andean subduction zone, Bolivia and Peru. *Journal of Geophysical Research*, **93**, 15,153–15,162.

HERMOZA, W. 2004. *Dynamique de tectono-sédimentaire et restauration séquentielle du rétro-bassin d'avant-pays des Andes centrales*. PhD thesis, Université Paul Sabatier-Toulouse III.

ISACKS, B. L. 1988. Uplift of the Central Andean plateau and bending of the Bolivian Orocline. *Journal of Geophysical Research*, **93**(B4), 3211–3231.

JAILLARD, E., HÉRAIL, G., MONFRET, T., DIAZ-MARTINEZ, BABY, P., LAVENU, A. & DUMONT, J.-F. 2000. Tectonic evolution of the Andes of Ecuador, Peru, Bolivia and northernmost Chile. *In*: CORDANI, U., MILANO, E. J., THOMAS FILHO, A. & CAMPOS, D. A. (eds) *Tectonic Evolution of South America. 31st International Geological Congress*, Rio de Janeiro, 481–559.

KETCHAM, R. A., DONELICK, R. A. & CARLSON, W. D. 1999. Variability of apatite fission track annealing kinetics III: Extrapolation to geological time scales. *American Mineralogist*, **84**, 1235–1255.

KETCHAM, R. A., DONELICK, R. A. & DONELICK, M. B. 2000. AFTSolve: A program for multi-kinetic

modelling of apatite fission-track data. *Geological Materials Research*, **2**(1), 32.

KONTAK, D. J., FARRAR, E. A., CLARK, A. H. & ARCHIBALD, D. A. 1990*a*. Eocene tectono-thermal rejuvenation of an upper Paleozoic–lower Mesozoic terrane in the Cordillera de Carabaya, Puno, south-eastern Peru, revealed by K–Ar and 40Ar/39Ar dating. *Journal of South American Earth Sciences*, **3**(4), 231–246.

KONTAK, D. J., FARRAR, E. A., CLARK, A. H., ARCHIBALD, D. A. & BAADSGAARD, H. 1990*b*. Late Paleozoic–early Mesozoic magmatism in the Cordillera de Carabaya, Puno, south-eastern Peru, geochronology and petrochemistry. *Journal of South American Earth Sciences*, **3**(4), 213–230.

LAMB, S. & DAVIS, P. 2003. Cenozoic climate change as a possible cause for the rise of the Andes. *Nature*, **425**, 792–797.

LAUBACHER, G. 1978. *Géologie de la Cordillière orientale et de l'Altiplano au nord et nord-ouest du Lac Titicaca (Pérou)*. Travaux et documents de l'ORSTOM, Paris, **95**.

MCQUARRIE, N., BARNES, J. B. & EHLERS, T. A. 2008. Geometric, kinematic, and erosional history of the central Andean Plateau, Bolivia (15–17S). *Tectonics*, **27**, TC3007, doi:10.1029/2006TC002054.

MÉGARD, F. 1984. The Andean orogenic period and its major structure in central and northern Peru. *Journal of the Geological Society, London*, **141**, 893–900.

NOBLE, D. C., MCKEE, E. H., EYZAGUIRRE, V. R. & MAROCCO, R. 1984. Age and regional tectonic and metallogenetic implications of igneous activity and mineralization in the Andahuaylas–Yauri belt of Southern Peru. *Economic Geology*, **79**, 172–176.

NORABUENA, E. O., DIXON, T. H., STEIN, S. & HARRISON, C. G. A. 1999. Decelerating Nazca–South America and Nazca–Pacific plate motions. *Geophysical Research Letters*, **26**, 3405–3408.

PARDO-CASAS, F. & MOLNAR, P. 1987. Relative motion of the Nazca (Farallon) and South American plate since Late Cretaceous times. *Tectonics*, **6**, 223–248.

PERELLO, J., CARLOTTO, V. *ET AL*. 2003. Porphyry-style alteration and mineralization of the Middle Eocene to Early Oligocene Andahuaylas–Yauri Belt, Cuzco region, Peru. *Economic Geology*, **98**, 1575–1605.

REINERS, P. W. & BRANDON, M. T. 2006. Using thermochronology to understand orogenic erosion. *Annual Reviews in Earth and Planetary Sciences*, **34**, 419–466.

ROPERCH, P., CARLOTTO, V. & CHAUVIN, A. 2008. Block rotations within the northern Peruvian Altiplano. *In*: *7th International Symposium on Andean Geodynamics (ISAG 2008, Nice), Extended Abstracts*, University of Nice, France, 469–472.

ROPERCH, P., SEMPERE, T. *ET AL*. 2006. Counterclockwise rotation of late Eocene-Oligocene fore-arc deposits in southern Peru and its significance for oroclinal bending in the central Andes. *Tectonics*, **25**, TC3010, doi:10.1029/2005TC001882.

ROUSSE, S., GILDER, S., FARBER, D., MCNULTY, B., PATRIAT, P., TORRES, V. & SEMPERE, T. 2003. Paleomagnetic tracking of mountain building in the Peruvian Andes since 10 Ma. *Tectonics*, **22**(5), 1048, doi:10.1029/2003TC001508.

ROUSSE, S., GILDER, S., FORNARI, M. & SEMPERE, T. 2005. Insight into the Neogene tectonic history of the northern Bolivian Orocline from new paleomagnetic and geochronologic data. *Tectonics*, **24**, TC6007, doi:10.1029/2004TC001760.

RUSSO, R. M. & SILVER, P. G. 1996. Cordillera formation, mantle dynamics, and the Wilson cycle. *Geology*, **24**(6), 511–514.

SCHILDGEN, T. F., HODGES, K. V., WHIPPLE, K. X., REINERS, P. W. & PRINGLE, M. S. 2007. Uplift of the western margin of the Andean plateau revealed from canyon incision history, southern Peru. *Geology*, **35**(6), 523–526.

SEMPERE, T., CARLIER, G. *ET AL*. 2002. Late Permian–Middle Jurassic lithospheric thinning in Peru and Bolivia, and its bearing on Andean-age tectonics. *Tectonophysics*, **345**, 153–181.

SEMPERE, T., HARTLEY, A. & ROPERCH, P. 2006. Comment on 'Rapid uplift of the altiplano revealed through C-13–O-18 bonds in paleosol carbonates'. *Science*, **314**(5800), 760.

STEINMANN, G. 1929. *Geologie von Peru*. Carl Winters Universitätsbuchhandlung, Heidelberg.

TAGAMI, T., CARTER, A. & HURFORD, A. J. 1996. Natural long-term annealing of the zircon fission-track system in Vienna Basin deep borehole samples: constraints upon the partial annealing zone and closure temperature. *Chemical Geology*, **130**, 147–157.

THOURET, J.-C., WÖRNER, G., GUNNEL, Y., SINGER, B., ZHANG, X. & SOURIOT, T. 2007. Geochronologic and stratigraphic constraints on canyon incision and Miocene uplift of the Central Andes in Peru. *Earth and Planetary Science Letters*, **263**, 151–166.